Next-to-leading order corrections to the gluon-induced forward jet vertex from the high energy effective action

G. Chachamis, M. Hentschinski, J. D. Madrigal Martínez, and A. Sabio Vera

NLO corrections to the gluon induced forward jet vertex from the high energy effective action

G. Chachamis[1], M. Hentschinski[2], J. D. Madrigal Martínez[3,4], A. Sabio Vera[3,4]

[1] Instituto de Física Corpuscular UVEG/CSIC, 46980 Paterna (Valencia), Spain.
[2] Department of Physics, Brookhaven National Laboratory, Upton, NY 11973, USA.
[3] Instituto de Física Teórica UAM/CSIC, Nicolás Cabrera 15, 28049 Madrid, Spain.
[4] Facultad de Ciencias, Universidad Autónoma de Madrid, C.U. Cantoblanco,
   28049 Madrid, Spain.

Abstract

We determine both real and virtual next-to-leading order corrections to the gluon induced forward jet vertex, from the high energy effective action proposed by Lipatov. For these calculations we employ the same regularization and subtraction formalism developed in our previous work on the quark-initiated vertex. We find agreement with previous results in the literature.

I Theoretical framework

In this work we present the calculation of the vertex describing the production of a jet in a forward direction very close in the detector to one of the hadrons in hadron-hadron interactions at very high energies. This is done in the kinematic approximation where the jet is well separated in rapidity from other jets also produced in the scattering process. As a calculational technique we make use of Lipatov's effective action [1], designed to easy the derivation of scattering amplitudes in the high energy limit of QCD. Here we focus on the gluon-initiated jet vertex, which is a more complicated counterpart of the quark-initiated vertex, derived with similar techniques in Ref. [2]. A convenient regularization and subtraction procedure, taken from Ref. [2], is shown to give the correct results (in agreement with previous calculations in the literature [3, 4, 5, 6, 7, 8]) at next-to-leading (NLO) accuracy. The convolution of this jet vertex with the NLO BFKL gluon Green function plays a very important role in the description of jet production at the LHC physics program. Many interesting studies have been performed in this direction in recent years, see Refs. [9, 10, 11, 12, 13, 14, 15, 16, 17, 18, 19, 20].

A complete description of the high energy effective action used in this work can be found in Refs. [1, 5]. For a more recent discussion directly related to our calculation we refer the reader to Ref. [22]. The calculation of the quark contributions to the gluon Regge trajectory at two loops

using Lipatov's effective action has been performed by us in Ref. [21, 23]. Here we will just briefly explain the general structure of this action to then describe in some detail our calculation of the gluon-initiated jet vertex.

The high energy effective action is based on the interplay between QCD particles and reggeized degrees of freedom, which are introduced as independent fields interacting with the standard ones via new vertices. These effective interactions, dominant in the high energy limit of QCD, appear inside an extra term added to the QCD action. Reggeized quarks and gluons "propagate" in the t-channel with modified propagators connecting two regions of different rapidities and play the role of suppressing any real emission in that interval. At the endpoints of these intervals there can be particle production; single production in multi-regge kinematics (MRK) and double production in quasi-multi-regge kinematics (QMRK). Within these clusters of particle production there are not kinematic restrictions and interactions are the usual QCD ones. A representation of this effective clustering is shown in Fig. 1.a. The ordering in rapidity of the produced clusters is of the form $y_0 \gg y_1 \gg \cdots \gg y_{n+1}$, where $y_k = \frac{1}{2} \ln \frac{k^+}{k^-}$ and with all particles in each cluster being emitted with a similar rapidity. Defining the light-cone vectors $n^{+,-} = 2p_{a,b}/\sqrt{s}$ we work with Sudakov expansions for four dimensional vectors of the form $k = \frac{1}{2}(k^+ n^- + k^- n^+) + \boldsymbol{k}$, with $\boldsymbol{k}$ being transverse. The strong ordering of the clusters simplifies the polarization tensor of the t-channel reggeized particles which can be written as $g_{\mu\nu} \to \frac{1}{2}(n^+)_\mu (n^-)_\nu + \mathcal{O}(\frac{1}{s})$, with $\sqrt{s}$ being the center-of-mass energy of the scattering process, carrying mainly transverse momenta, $q_i^2 = -\boldsymbol{q}_i^2$.

(a)   (b)
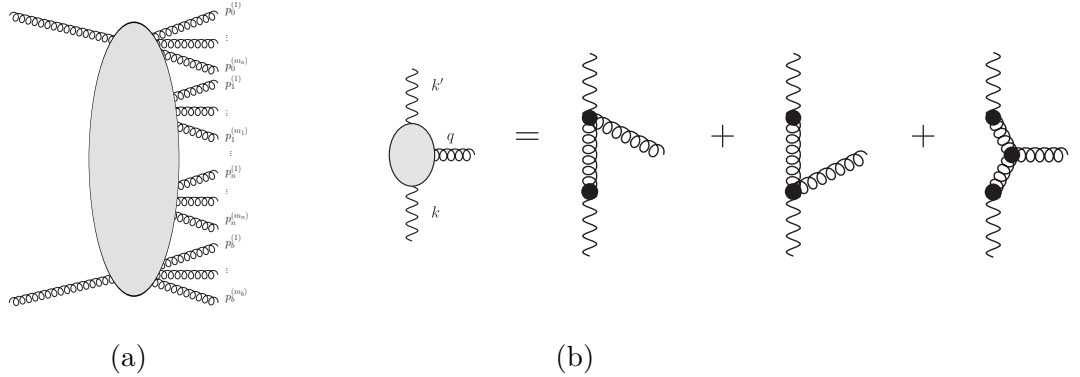
Figure 1: *(a) Quasi-multi-regge kinematics; (b) reggeized gluon-reggeized gluon-gluon effective vertex. The first two diagrams are the induced contributions.*
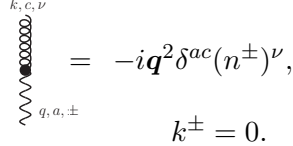
The effective interaction between reggeized and usual particles, like the one shown in Fig. 1, consists of two pieces: the projection of the QCD vertex onto high energy kinematics and additional induced contributions. This structure can be obtained from the following form of the effective action:

$$S_{\text{eff}} = S_{\text{QCD}} + S_{\text{ind}}; \quad S_{\text{ind}} = \int d^4x \, \text{Tr}[(W_+[v(x)] - \mathscr{A}_+(x))\partial_\perp^2 \mathscr{A}_-(x)] + \{+ \leftrightarrow -\}, \quad (1)$$

where $\mathscr{A}_\pm$ are the gauge-invariant reggeized gluon fields which satisfy the following kinematic constraint

$$\partial_+ \mathscr{A}_-(x) = 0 = \partial_- \mathscr{A}_+(x). \quad (2)$$
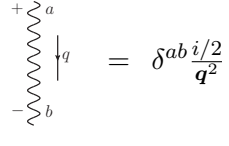
Their couplings to the QCD gluon field is given in terms of two non-local functionals $W_\pm[v] = v_\pm \frac{1}{D_\pm}\partial_\pm = v_\pm - g v_\pm \frac{1}{\partial_\pm} v_\pm + \cdots$ with $D_\pm = \partial_\pm + g v_\pm$.

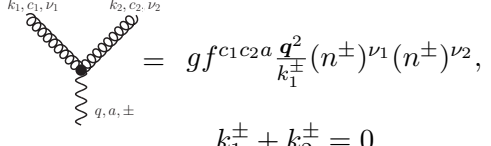$$= -i\boldsymbol{q}^2 \delta^{ac}(n^\pm)^\nu, \qquad = \delta^{ab}\frac{i/2}{\boldsymbol{q}^2} \qquad = g f^{c_1 c_2 a}\frac{\boldsymbol{q}^2}{k_1^\pm}(n^\pm)^{\nu_1}(n^\pm)^{\nu_2},$$

$$k^\pm = 0. \qquad\qquad\qquad\qquad k_1^\pm + k_2^\pm = 0$$
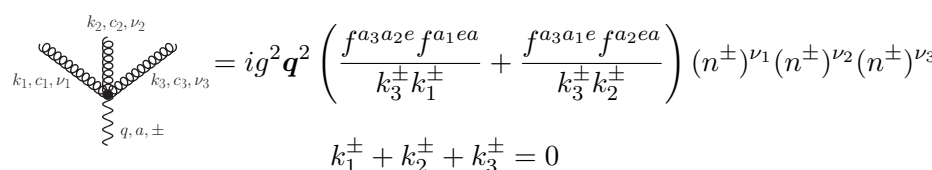
$$\text{(a)}\qquad\qquad\qquad\text{(b)}\qquad\qquad\qquad\text{(c)}$$

$$= ig^2\boldsymbol{q}^2\left(\frac{f^{a_3 a_2 e}f^{a_1 ea}}{k_3^\pm k_1^\pm} + \frac{f^{a_3 a_1 e}f^{a_2 ea}}{k_3^\pm k_2^\pm}\right)(n^\pm)^{\nu_1}(n^\pm)^{\nu_2}(n^\pm)^{\nu_3}$$

$$k_1^\pm + k_2^\pm + k_3^\pm = 0$$

$$\text{(d)}$$

Figure 2: *Feynman rules for the lowest-order effective vertices. Wavy lines denote reggeized fields and curly lines gluons. (a) is the direct transition vertex and (b) the reggeized gluon propagator. We also show the unregulated order g (c) and order g^2 (d) induced vertices.*

The lowest order Feynman rules for the induced vertices are shown in Fig. 2. The contributions in the vertices of the form $1/k^\pm$ generate a new type of divergencies which will be related to high energy logarithms. These divergencies call for a regularization, or equivalently, a suitable definition of the nonlocal operator $\partial_\pm^{-1}$ in the Wilson lines. A convenient regularization scheme was defined in [2, 21] where n^+ and n^- are replaced by tilted light-cone vectors of the form $a = n^- + e^{-\rho}n^+$ and $b = n^+ + e^{-\rho}n^-$. These tilted light-cone vectors form a hyperbolic angle ρ in Minkowski space which can be interpreted as $\ln s$, implying that at high energies we are interested in the $\rho \to \infty$ limit. In the following we treat ρ as an external parameter which, at the end, we consider in the $\rho \to \infty$ limit, similar to the treatment of $\epsilon \to 0$ in $d = 4 + 2\epsilon$ dimensional regularization.

After this brief Introduction we turn in the following to give details of our calculation of the gluon-initiated forward jet vertex. In Section II we provide a description of the virtual corrections to the gluon-gluon-reggeized gluon vertex, while in Section III we explain the key details for the calculation of the real corrections. Finally, Section IV contains our conclusions and an outlook for future calculations. The Appendix collects further technical details.

II Virtual Corrections to the Gluon-Gluon-Reggeized Gluon Vertex

Let us consider the process $gg \to gg$, where the external gluons are on-shell: $p_a^2 = (p_a - q)^2 = p_b^2 = (p_b + q)^2 = 0$. In the high-energy limit the corresponding scattering amplitude factorizes into a reggeized gluon exchange in the t-channel and its couplings to the external particles, the so-called

impact factors. At tree level this is shown in Fig. 3.

Light cone momenta are defined making use of the momenta of the incoming particles p_a and p_b through $p_a = p_a^+ n^-/2$ and $p_b = p_b^- n^+/2$ with $2p_a \cdot p_b = s = p_a^+ p_b^-$. From Eq. (2) one obtains for the upper vertex the constraint $q^+ = 0$, while $q^- = 0$ for the lower one. Both constraints can be understood as the leading term in the expansion in the small q^+/p_a^+ and q^-/p_b^- ratios, respectively. The polarization vectors must be physical, satisfying for the upper vertex $\varepsilon \cdot p_a = 0$ and $\varepsilon^* \cdot (p_a - q) = 0$. The last relation implies that $\varepsilon^* \cdot p_a = \varepsilon^* \cdot q$. Gauge invariance of the effective action enables us to choose *different* gauges for the upper and lower gluon-gluon-reggeized gluon couplings. We therefore impose the condition $\varepsilon(p_a) \cdot n^+ = \varepsilon^*(p_1) \cdot n^+ = 0$ for the upper vertex and the condition $\varepsilon(p_b) \cdot n^- = \varepsilon^*(p_2) \cdot n^- = 0$ for the lower vertex, which implies the following polarization sum

$$\sum_{\text{polarizations}} \varepsilon_\mu^\lambda(p, n)(\varepsilon_\nu^{\lambda'})^*(p, n) = -g_{\mu\nu} + \frac{p_\mu n_\nu + p_\nu n_\mu}{p \cdot n}, \tag{3}$$

with p being the gluon momentum and $n = n^\pm$.
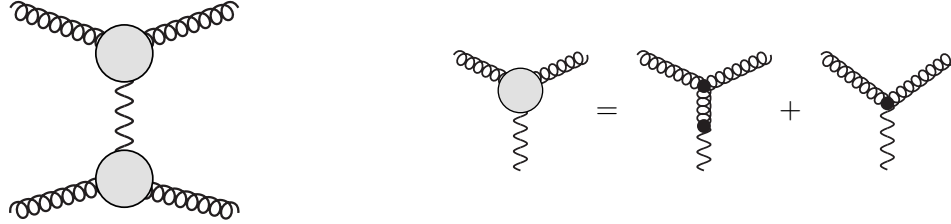
Figure 3: *Tree-level contribution to the gluon-gluon scattering amplitude in terms of effective vertices.*

To define the impact factors we start from the general definition for the differential cross-section for m-particle production in terms of the corresponding matrix elements and the phase space integral, *i.e.*

$$d\sigma = \frac{1}{2s}|\mathcal{M}_{i \to f}|^2 d\Pi_m (2\pi)^d \delta^d\left(p_a + p_b - \sum_{j=1}^m p_j\right); \quad d\Pi_m = \prod_{j=1}^m \frac{d^d p_j}{(2\pi)^{d-1}} \delta_+(p_j^2). \tag{4}$$

In the special case where all final state particles are produced either in the fragmentation region of particle a or particle b we rewrite, with $m = m_a + m_b$, the overall delta function for global momentum conservation as follows

$$(2\pi)^d \delta^d\left(p_a + p_b - \sum_{j=1}^m p_j\right) = \int \frac{d^d k}{(2\pi)^d} (2\pi)^{2d} \delta^d\left(p_a + k - \sum_{j=1}^{m_a} p_j\right) \times \delta^d\left(p_b - k - \sum_{l=1}^{m_b} p_j\right). \tag{5}$$

The generalization to the additional production of n-particle clusters at central rapidities (see also Fig. 1.a), with $m = m_a + m_b + \sum_i^n m_i$, reads

$$(2\pi)^d \delta^d\left(p_1 + p_2 - \sum_{j=1}^m p_j\right) = \prod_{i=0}^n \int \frac{d^d k_i}{(2\pi)^d} (2\pi)^{(2+n)d} \delta^d\left(p_a + k_0 - \sum_{l_0=1}^{m_a} p_{l_0}\right) \times$$

$$\delta^d\left(p_b - k_n - \sum_{l_n=1}^{m_b} p_j\right) \times (2\pi)^{nd} \delta^d\left(k_0 - k_1 - \sum_{l_1=1}^{m_1} p_{l_1}\right) \times \ldots \delta^d\left(k_{n-1} - k_n - \sum_{l_n=1}^{m_n} p_{l_n}\right). \tag{6}$$

4

Restricting from now on to the $gg \to gg$ amplitude at tree-level, we use in our next step the fact that the effective action naturally factorizes the amplitude $i\mathcal{M}_{gr^* \to g_1}$ into two products of $i\mathcal{M}_{gr^* \to g_1}$ times the square-root of the reggeized gluon propagator $i/2\boldsymbol{q}^2$. Squaring, averaging over color and polarization of the initial gluon and summing over color and polarization of the final state and reggeized gluon (at the level of the $gr^* \to g$ amplitudes), the $2 \to 2$ tree-level amplitude takes the following factorized form

$$\overline{|\mathcal{M}_{g_a g_b \to g_1 g_2}^{(0)}|^2} = \frac{\overline{|\mathcal{M}_{g_a r^* \to g_1}^{(0)}|^2}}{2\boldsymbol{k}^2\sqrt{N_c^2 - 1}} \times \frac{\overline{|\mathcal{M}_{g_b r^* \to g_2}^{(0)}|^2}}{2\boldsymbol{k}^2\sqrt{N_c^2 - 1}}. \tag{7}$$

Defining now the impact factors $= h_{a,b}^{(0)}(\boldsymbol{q})$ through the relation

$$d\sigma_{ab} = h_a^{(0)}(\boldsymbol{k}) h_b^{(0)}(\boldsymbol{k}) d^{2+2\epsilon}\boldsymbol{k}, \tag{8}$$

we are lead to the following general expression in terms of the effective action matrix elements:

$$h_{a,\text{gluon}}^{(0)}(\boldsymbol{k}) = \frac{(2\pi)^{d/2}}{2p_a^+} \int dk^- \frac{\overline{|\mathcal{M}_{g_a r^* \to g_1}^{(0)}|^2}}{2\boldsymbol{k}^2\sqrt{N_c^2 - 1}} d\Pi_1 \delta^{(d)}(p_a + k - p_1), \tag{9}$$

with a natural generalization to m_b-particle production in the fragmentation region of particle b. The $i\mathcal{M}_{gr^* \to g_1}$ amplitude itself receives at tree-level two contributions (see Fig. 3): one from the gluon-gluon-reggeized gluon (GGR) vertex

$$g f_{abc} \frac{\boldsymbol{k}^2}{p_a^+} (n^+)^{\mu_1} (n^+)^{\mu_2} \varepsilon_{\mu_1} \varepsilon_{\mu_2}^*$$

and the other from the projection of the 3-gluon vertex

$$g f_{abc} \left[2g^{\mu_1 \mu_2} p_a^+ - (n^+)^{\mu_1} (p_a - k)^{\mu_2} - (n^+)^{\mu_2} (2k + p_a)^{\mu_1} \right] \varepsilon_{\mu_1} \varepsilon_{\mu_2}^*.$$

It is possible to verify that this amplitude is gauge invariant and satisfies the necessary Ward/Slavnov-Taylor identities, see *e.g.* [1, 22]. At the amplitude level we arrive at

$$\mathcal{M}_{g_a r^* \to g_1} = 2g f_{abc} \epsilon \cdot \epsilon^*. \tag{10}$$

and

$$h_{a,\text{gluon}}^{(0)}(\boldsymbol{k}) = \frac{N_c}{\sqrt{N_c^2 - 1}} \frac{g^2}{\boldsymbol{k}^2} \frac{1}{(2\pi)^{1+\epsilon}} = \frac{2^{1+\epsilon}\alpha_s C_A}{\mu^{2\epsilon}\Gamma(1-\epsilon)\sqrt{N_c^2 - 1}} \frac{1}{\boldsymbol{k}^2}; \qquad \alpha_s \equiv \frac{g^2 \mu^{2\epsilon}\Gamma(1-\epsilon)}{(4\pi)^{1+\epsilon}}. \tag{11}$$

The one-loop corrections to this gluon-gluon-reggeized gluon vertex are shown in Fig. 4. All diagrams are evaluated in the limit $\rho \to \infty$, while we only keep track of divergent ($\mathcal{O}(\rho)$) and finite ($\mathcal{O}(\rho^0)$) terms; ϵ is on the other hand kept finite. Details about the calculation of individual diagrams can be found in the appendix A.1. The final result for the 1-loop $gr^* \to g$ amplitude
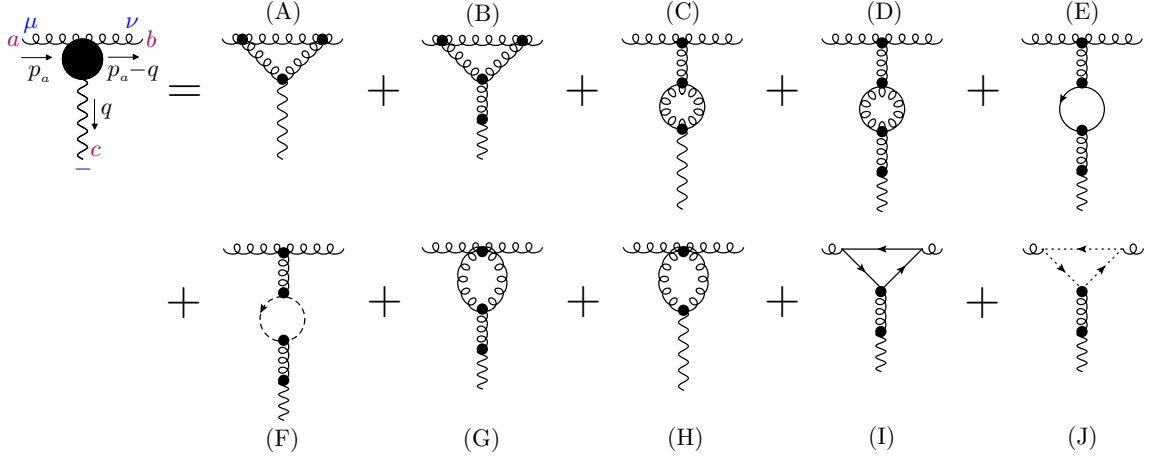
Figure 4: *One-loop virtual corrections to the gluon-initiated jet vertex.*

reads

$$
i\mathcal{M}^{(1)}_{g_a r^* \to g_1} = -\frac{g^3 \mu^{2\epsilon} p_a^+}{(4\pi)^{2+\epsilon}} f_{abc} \left(\frac{\boldsymbol{k}^2}{\mu^2}\right)^{\epsilon} \left\{ N_c\, \varepsilon \cdot \varepsilon^* \frac{\Gamma(1-\epsilon)\Gamma^2(\epsilon)}{\Gamma(2\epsilon)} \left[2\ln\left(\frac{p_a^+}{|\boldsymbol{k}|}\right) + \rho + \psi(1) \right.\right.
$$
$$
\left. - 2\psi(\epsilon) + \psi(1-\epsilon) \right] + 8[N_c(1+\epsilon) - n_f]\left[-\frac{1}{2}\varepsilon \cdot \varepsilon^* \frac{\Gamma^2(1+\epsilon)\Gamma(-\epsilon)}{\Gamma(4+2\epsilon)} \right.
$$
$$
\left. + \frac{\varepsilon \cdot q\, \varepsilon^* \cdot q}{\boldsymbol{k}^2} \frac{\Gamma(\epsilon)\Gamma(1-\epsilon)}{\Gamma(4+2\epsilon)} (2\Gamma(1+\epsilon) + \Gamma(2+\epsilon)) \right]
$$
$$
+ 8[N_c(1+\epsilon) - n_f]\frac{\varepsilon \cdot q\, \varepsilon^* \cdot q}{\boldsymbol{k}^2} \frac{\Gamma(-\epsilon)\Gamma^2(1+\epsilon)}{(2+2\epsilon)\Gamma(2+2\epsilon)} + \varepsilon \cdot \varepsilon^* (4N_c - n_f)\frac{\Gamma(-\epsilon)\Gamma^2(1+\epsilon)}{\epsilon\,\Gamma(2+2\epsilon)}
$$
$$
- \varepsilon \cdot \varepsilon^* (4N_c - n_f)\frac{1+2\epsilon}{\epsilon} \frac{\Gamma(-\epsilon)\Gamma^2(1+\epsilon)}{\Gamma(2+2\epsilon)} + 2N_c\, \varepsilon \cdot \varepsilon^* \frac{\Gamma(-\epsilon)\Gamma^2(1+\epsilon)}{\Gamma(2+2\epsilon)}
$$
$$
+ 2\,\varepsilon \cdot \varepsilon^* [(1+\epsilon)N_c - n_f]\frac{\Gamma(-\epsilon)\Gamma^2(1+\epsilon)}{(3+2\epsilon)\Gamma(2+2\epsilon)} - 2\varepsilon \cdot \varepsilon^* [4N_c - n_f]\frac{\Gamma(-\epsilon)\Gamma^2(1+\epsilon)}{\Gamma(2+2\epsilon)} \right\}. \tag{12}
$$

Our result contains two types of tensor structures involving the initial and final polarization tensors, namely, $\varepsilon \cdot \varepsilon^*$ and $\varepsilon \cdot q\, \varepsilon^* \cdot q/\boldsymbol{k}^2$. These are related to the helicity conserving and helicity violating terms [8]

$$
\varepsilon \cdot \varepsilon^* = \delta_{\lambda_a, \lambda_1}; \qquad \varepsilon \cdot \varepsilon^* + \frac{2}{\boldsymbol{k}^2}\varepsilon \cdot q\, \varepsilon^* \cdot q = -\delta_{\lambda_a, -\lambda_1}. \tag{13}
$$

To avoid double counting it is now needed to introduce the subtraction procedure discussed in the Introduction. This procedure requires to subtract all effective diagrams which contain internal reggeized gluon propagators in the t-channel from the above result. With

$$
= i\mathcal{M}^{(1)}_{g_a r^* \to g_1}, \tag{14}
$$

6

the subtraction procedure results into the following coefficient

$$
\mathcal{C}_{gr^* \to g}\left(\frac{p_a^+}{\sqrt{\boldsymbol{k}^2}}, \rho; \epsilon \frac{\boldsymbol{k}^2}{\mu^2}\right) = \quad \text{(diagram)} \quad = \quad \text{(diagram)} \quad - \quad \text{(diagram)} \quad . \tag{15}
$$

The one-loop reggeized gluon self-energy, which was computed in [2], includes both divergent, $\mathcal{O}(\rho)$, and finite terms of $\mathcal{O}(\rho^0)$ and reads[1]

$$
\Sigma^{(1)}\left(\rho; \epsilon, \frac{\boldsymbol{k}^2}{\mu^2}\right) = \quad \text{(diagram)} \quad = (-2i\boldsymbol{k}^2)\,\omega^{(1)}(\boldsymbol{k}^2)\left[\rho - \frac{i\pi}{2} + \frac{5 + 3\epsilon - \frac{n_f}{N_c}(2 + 2\epsilon)}{2(1 + 2\epsilon)(3 + 2\epsilon)}\right]. \tag{16}
$$

where

$$
\omega^{(1)}(\boldsymbol{k}^2) = -\frac{\alpha_s N_c}{2\pi}\frac{\Gamma^2(1 + \epsilon)}{\epsilon\Gamma(1 + 2\epsilon)}\left(\frac{\boldsymbol{k}^2}{\mu^2}\right)^\epsilon \tag{17}
$$

is the one-loop gluon Regge trajectory. The high energy limit of the gluon-gluon scattering amplitude at one-loop is then obtained as the following sum of diagrams

$$
\text{(diagram)} \quad = \quad \text{(diagram)} \quad + \quad \text{(diagram)} \quad + \quad \text{(diagram)} \tag{18}
$$

While each diagram on the right side is divergent in the limit $\rho \to \infty$, the divergence cancels in their sum, resulting into a finite one-loop amplitude. Following [21] we therefore define renormalized gluon-gluon-reggeized gluon coupling coefficients,

$$
\mathcal{C}_{gr^* \to g}^{\mathrm{R}}\left(\frac{p_a^+}{M^+}; \epsilon, \frac{\boldsymbol{q}^2}{\mu^2}\right) = Z^+\left(\frac{M^+}{\sqrt{\boldsymbol{k}^2}}, \rho; \epsilon, \frac{\boldsymbol{k}^2}{\mu^2}\right)\mathcal{C}_{gr^* \to g}\left(\frac{p_a^+}{\sqrt{\boldsymbol{k}^2}}, \rho; \epsilon\frac{\boldsymbol{k}^2}{\mu^2}\right), \tag{19}
$$

$$
\mathcal{C}_{gr^* \to g}^{\mathrm{R}}\left(\frac{p_b^-}{M^-}; \epsilon, \frac{\boldsymbol{k}^2}{\mu^2}\right) = Z^-\left(\frac{M^-}{\sqrt{\boldsymbol{k}^2}}, \rho; \epsilon, \frac{\boldsymbol{k}^2}{\mu^2}\right)\mathcal{C}_{gr^* \to g}\left(\frac{p_b^-}{\sqrt{\boldsymbol{k}^2}}, \rho; \epsilon\frac{\boldsymbol{k}^2}{\mu^2}\right), \tag{20}
$$

and the renormalized reggeized gluon propagator,

$$
G^{\mathrm{R}}\left(M^+, M^-; \epsilon, \boldsymbol{k}^2, \mu^2\right) = \frac{G\left(\rho; \epsilon, \boldsymbol{k}^2, \mu^2\right)}{Z^+\left(\frac{M^+}{\sqrt{\boldsymbol{k}^2}}, \rho; \epsilon, \frac{\boldsymbol{k}^2}{\mu^2}\right)Z^-\left(\frac{M^-}{\sqrt{\boldsymbol{k}^2}}, \rho; \epsilon, \frac{\boldsymbol{k}^2}{\mu^2}\right)}, \tag{21}
$$

---

[1]There is a misprint in [2]: the term $[\cdots]_2$ in Eq. 6 of [2] vanishes. As the same contribution appears also in the 1-loop corrections to the quark-quark-reggeized gluon vertex, the final result is independent of this contribution and remains unchanged.

with the bare reggeized gluon propagator given by

$$G\left(\rho;\epsilon,\boldsymbol{k}^2,\mu^2\right) = \frac{i/2}{\boldsymbol{k}^2}\left\{1 + \frac{i/2}{\boldsymbol{k}^2}\Sigma\left(\rho;\epsilon,\frac{\boldsymbol{k}^2}{\mu^2}\right) + \left[\frac{i/2}{\boldsymbol{k}^2}\Sigma\left(\rho;\epsilon,\frac{\boldsymbol{k}^2}{\mu^2}\right)\right]^2 + \dots\right\}. \tag{22}$$

The renormalization factors $Z^{\pm}$ cancel for the complete scattering amplitude and can be parametrized as follows

$$Z^{\pm}\left(\frac{M^{\pm}}{\sqrt{\boldsymbol{k}^2}},\rho;\epsilon,\frac{\boldsymbol{k}^2}{\mu^2}\right) = \exp\left[\left(\rho - \ln\frac{M^{\pm}}{\sqrt{\boldsymbol{k}^2}}\right)\omega\left(\epsilon,\frac{\boldsymbol{k}^2}{\mu^2}\right) + f^{\pm}\left(\epsilon,\frac{\boldsymbol{k}^2}{\mu^2}\right)\right], \tag{23}$$

where the gluon Regge trajectory has the following perturbative expansion,

$$\omega\left(\epsilon,\frac{\boldsymbol{k}^2}{\mu^2}\right) = \omega^{(1)}\left(\epsilon,\frac{\boldsymbol{k}^2}{\mu^2}\right) + \omega^{(2)}\left(\epsilon,\frac{\boldsymbol{k}^2}{\mu^2}\right) + \dots, \tag{24}$$

with the one-loop expression given in Eq. (17). The function $f(\epsilon,\boldsymbol{k}^2)$ parametrizes finite contributions and is, in principle, arbitrary. While symmetry of the scattering amplitude requires $f^+ = f^- = f$, Regge theory suggests to fix it in such a way that at one loop the non-ρ-enhanced contributions of the one-loop reggeized gluon self energy are entirely transferred to the quark-reggeized gluon couplings. This leads to

$$f^{(1)}\left(\epsilon,\frac{\boldsymbol{k}^2}{\mu^2}\right) = -\frac{\alpha_s N_c \Gamma^2(1+\epsilon)}{4\pi\Gamma(1+2\epsilon)}\left(\frac{\boldsymbol{q}^2}{\mu^2}\right)^{\epsilon}\left[\frac{5 + 3\epsilon - \frac{n_f}{N_c}(2+2\epsilon)}{2(1+2\epsilon)(3+2\epsilon)}\right]. \tag{25}$$

Let us remark that in principle other alternative and even asymmetric $f^+ \neq f^-$ choices are possible, as long as they are in agreement with UV-renormalizability of QCD and collinear factorization. Using now $M^+ = p_a^+$, $M^- = p_b^-$ we can see that this choice for f keeps the full s-dependence of the amplitude inside the reggeized gluon exchange. The renormalized gluon-gluon-reggeized gluon couplings allows then to extract the NLO corrections to the gluon impact factor. Extracting the Born contribution and decomposing into helicity conserving and non-conserving parts

$$\mathcal{C}_{gr^*\to g}^{\mathrm{R}}\left(1;\epsilon,\frac{\boldsymbol{q}^2}{\mu^2}\right) = 2g f_{abc}\cdot\left[\Gamma_a^{(+)}\delta_{\lambda_a,\lambda_1} + \Gamma_a^{(-)}\delta_{\lambda_a,-\lambda_1}\right], \tag{26}$$

where the helicity tensors are for finite ϵ defined through Eq. (13), we have

$$\Gamma_a^{(+)} = -\frac{1}{2}\omega^{(1)}\left[-\psi(1) + 2\psi(2\epsilon) - \psi(1-\epsilon) + \frac{1}{4(1+2\epsilon)(3+2\epsilon)} + \frac{7}{4(1+2\epsilon)} - \frac{n_f}{N_c}\frac{1+\epsilon}{(1+2\epsilon)(3+2\epsilon)}\right]$$

$$= \frac{\alpha_s N_c}{4\pi}\left(\frac{\boldsymbol{q}^2}{\mu^2}\right)^{\epsilon}\left[-\frac{1}{\epsilon^2} + \frac{\beta_0}{2\epsilon} - \frac{(67-\pi^2)N_c - 10 n_f}{18}\right] + \mathcal{O}(\epsilon), \qquad \beta_0 = \frac{11}{3}N_c - \frac{2}{3}n_f;$$

$$\Gamma_a^{(-)} = -\frac{1}{2}\omega^{(1)}\left[\frac{\epsilon}{(1+\epsilon)(1+2\epsilon)(3+2\epsilon)}\left(1 + \epsilon - \frac{n_f}{N_c}\right)\right] = \frac{\alpha_s}{12\pi}(N_c - n_f) + \mathcal{O}(\epsilon). \tag{27}$$

which is in precise agreement with the literature [2] [3, 4, 5, 6, 8].

---

[2] As noted in [6], the original result [3] contains several misprints. The correct expressions can be found *e.g.* in [5, 6, 8].

III   Real Corrections and One-Loop Jet Vertex

In the high energy limit, the real corrections to the Born-level process are naturally cast into three contributions to the $gg \to ggg$ amplitude where the additional gluon is either produced at central rapidities or close to the fragmentation region of one of the initial gluons (quasi-elastic gluon production), see Fig. 5. A second class of corrections is due to the possible fragmentation of one of the initial gluons into a $q\bar{q}$ pair which only contributes to the quasi-elastic region, see Fig. 6.
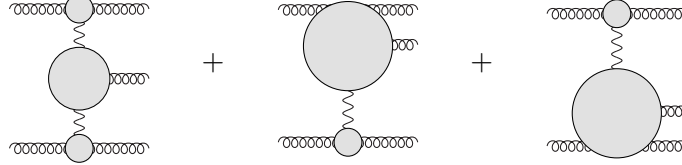
Figure 5: *Central (left) and quasi-elastic (middle and right) gluon production.*
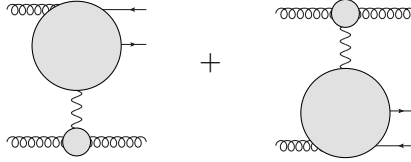
Figure 6: *Quark production is restricted to the quasi-elastic region.*

In the same way as the effective action generates high energy divergences near the light-cone when computing virtual corrections, a cut-off in rapidity must be enforced in the longitudinal integrations.

The central production amplitude yields the unintegrated real part of the forward leading order BFKL kernel and is obtained from the sum of the following three effective diagrams:

$$\qquad (28)$$

The squared amplitude for (28), averaged over color of the incoming reggeized fields and summed over final state color and helicities reads [2]

$$\overline{|\mathcal{M}|^2}_{r^*r^* \to g} = \frac{16g^2 N_c}{N_c^2 - 1} \frac{\boldsymbol{k'}^2 \boldsymbol{k}^2}{\boldsymbol{q}^2} \qquad (29)$$

with $\boldsymbol{k}' = \boldsymbol{k} - \boldsymbol{q}$. Defining the central production vertex $V^{(0)}$ through the differential cross section[3],

$$d\hat{\sigma}_{ab}^{(c)} = h_a^{(0)}(\boldsymbol{k}')h_b^{(0)}(\boldsymbol{k})\mathcal{V}(\boldsymbol{k}, \boldsymbol{k}'; \boldsymbol{q})d^{2+2\epsilon}\boldsymbol{k}'\, d^{2+2\epsilon}\boldsymbol{k}\, dy, \qquad (30)$$

we obtain, using the decomposition in Eq. (6) and with $\mu^2 = k^{+'}k^-$:

$$V(\boldsymbol{k}, \boldsymbol{k}'; \boldsymbol{q}) = \frac{N_c^2 - 1}{8} \int d\mu^2 \frac{\overline{|\mathcal{M}|^2}_{r^*r^* \to g}}{\boldsymbol{k}^2 \boldsymbol{k}'^2} d\Pi_1 \delta^{(d)}(k' - k - q)$$

$$= \frac{\alpha_s N_c}{\pi_\epsilon \pi \boldsymbol{q}^2}; \qquad\qquad \pi_\epsilon \equiv \pi^{1+\epsilon}\Gamma(1 - \epsilon)\mu^{2\epsilon}. \qquad (31)$$

While the rapidities of the gluons in the forward and backward directions are determined by kinematics, $y_a = \ln p_a^+/|\boldsymbol{k}'|$ and $y_b = -\ln p_b^-/|\boldsymbol{k}|$, the integral over the gluon rapidity in Eq. (30) leads to a divergence in the limit $y \to \pm\infty$ of inclusive observables. We therefore introduce upper and lower bounds $\eta_{a,b}$ on this integral with $\eta_a > y > \eta_b$ which we evaluate in the limit $\eta_{a,b} \to \pm\infty$. This leads then to the definition of the regularized production vertex $\mathcal{V}(\boldsymbol{k}, \boldsymbol{k}'; \boldsymbol{q}; \eta_a, \eta_b) \equiv V(\boldsymbol{k}, \boldsymbol{k}')\Theta(\eta_a - y)\Theta(y - \eta_b)$.

The remaining part of our calculation, the quasi-elastic contribution $g(p_a)r^*(k) \to g(p)g(q)$ (see the notation in Fig. 7), is given by the sum of all the effective diagrams in Fig. 8, where we include both the gg and the $q\bar{q}$ final state. In the computation of these diagrams we will employ the
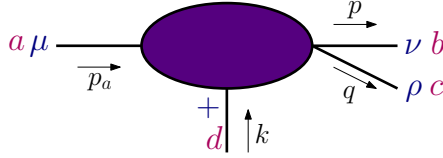
**Figure 7:** *Notation for external momenta and color indices in the quasi-elastic contribution.*

following choice for the polarization vectors: $\varepsilon_a \cdot p_a = \varepsilon_b \cdot p = \varepsilon_c \cdot q = \varepsilon_a \cdot n^+ = \varepsilon_b \cdot n^+ = \varepsilon_c \cdot n^+ = 0$; together with the Sudakov decomposition

$$p_a = p_a^+ \frac{n^-}{2}, \qquad p = (1 - z)p_a^+ \frac{n^-}{2} + p^- \frac{n^+}{2} + \boldsymbol{k}',$$
$$k = k^- \frac{n^+}{2} + \boldsymbol{k}, \qquad q = zp_a^+ \frac{n^-}{2} + (k^- - p^-)\frac{n^+}{2} + \boldsymbol{q}, \qquad (32)$$

where we used $q^+ = zp_a^+$ and $p_a^+ = (1 - z)p_a^+$. Squaring and averaging over initial colors and polarizations and summing over the final state we obtain with $\boldsymbol{\Delta} = \boldsymbol{q} - z\boldsymbol{k}$

$$\overline{|\mathcal{M}^2|}_{gg \to ggg} =$$

$$8z(1 - z)(p_a^+)^2 g^4 C_a(1 + \epsilon)\mathcal{P}_{gg}(z)\frac{k^2}{\boldsymbol{k}'^2}\left[\frac{z^2 \boldsymbol{k}'^2 + (1 - z)^2 \boldsymbol{q}^2 - z(1 - z)\boldsymbol{q} \cdot \boldsymbol{k}'}{\boldsymbol{q}^2 \boldsymbol{\Delta}^2}\right], \qquad (33)$$

---

[3]Strictly speaking we cannot identify the gluon with transverse momentum $\boldsymbol{q} = \boldsymbol{k} - \boldsymbol{k}'$ to be the centrally produced one. The cross-section should be therefore written as the sum over the three possibilities where one of the gluons is produced at central rapidities, together with the corresponding symmetry factor $1/3$.
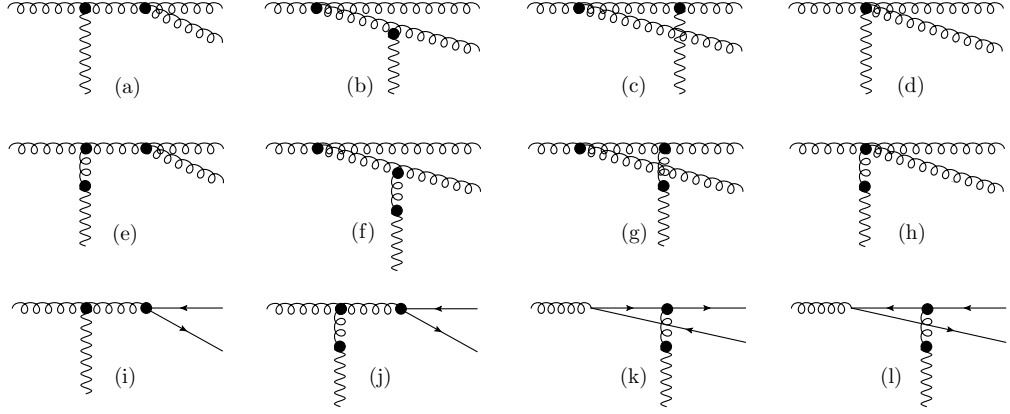
Figure 8: *Diagrams involved in the computation of the real corrections. In the case of final $q\bar{q}$ state, the external quark has momentum p and the external antiquark momentum q.*

where $\mathcal{P}_{gg}(z) = C_a \frac{1+z^4+(1-z)^4}{z(1-z)}$ is the gluon-gluon Altarelli-Parisi splitting function. In the same way, the joined contribution of the diagrams (j), (k) and (l) for the quark-antiquark final state gives

$$\overline{|\mathcal{M}^2|}\Big|_{gg \to q\bar{q}} = 8z(1-z)(p_a^+)^2 g^4 n_f N_c (1+\epsilon) \mathcal{P}_{qg}(z,\epsilon) \frac{\boldsymbol{k}^2}{\boldsymbol{q}^2 \boldsymbol{k}'^2} \left[\frac{C_f}{C_a} + z(1-z) \frac{\boldsymbol{q} \cdot \boldsymbol{\Delta}}{\boldsymbol{\Delta}^2} \right], \tag{34}$$

with $\mathcal{P}_{qg}(z,\epsilon) = \frac{1}{2} \left[1 - \frac{2z(1-z)}{1+\epsilon} \right]$ the quark-gluon splitting function. Generalizing our definition in Eq. (9) to two final state particles we obtain

$$\begin{aligned} h_{a,gg}^{(1)}(\boldsymbol{k}) &= \frac{(2\pi)^{d/2}}{2p_a^+} \int dk^- \frac{\overline{|\mathcal{M}_{g_a r^* \to gg}^{(0)}|^2}}{2\boldsymbol{k}^2 \sqrt{N_c^2 - 1}} d\Pi_2 \delta^{(d)}(p_a + k - p - q) \\ &= \int dz d^{2+2\epsilon} \boldsymbol{k}' F_{ggg}(\boldsymbol{k}, \boldsymbol{k}', z) h_{a,\text{gluon}}^{(0)}(\boldsymbol{k}') \end{aligned} \tag{35}$$

and

$$\begin{aligned} h_{a,q\bar{q}}^{(1)}(\boldsymbol{k}) &= \frac{(2\pi)^{d/2}}{2p_a^+} \int dk^- \frac{\overline{|\mathcal{M}_{g_a r^* \to gg}^{(0)}|^2}}{2\boldsymbol{k}^2 \sqrt{N_c^2 - 1}} d\Pi_2 \delta^{(d)}(p_a + k - p - q) \\ &= \int dz d^{2+2\epsilon} \boldsymbol{k}' F_{gq\bar{q}}(\boldsymbol{k}, \boldsymbol{k}', z) h_{a,\text{gluon}}^{(0)}(\boldsymbol{k}') \end{aligned} \tag{36}$$

with

$$F_{ggg}(\boldsymbol{k}, \boldsymbol{k}', z) = \frac{1}{2} \frac{\alpha_s}{2\pi \pi_\epsilon} \mathcal{P}_{gg}(z) \left[\frac{z^2 \boldsymbol{k}'^2 + (1-z)^2 \boldsymbol{q}^2 - z(1-z)\boldsymbol{q} \cdot \boldsymbol{k}'}{\boldsymbol{q}^2 \boldsymbol{\Delta}^2} \right] \tag{37}$$

and
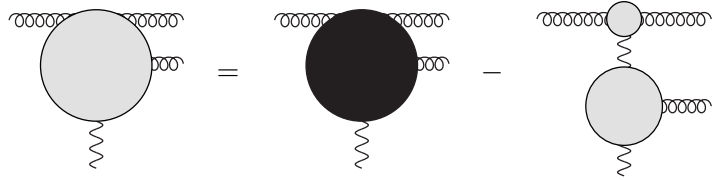
$$F_{gq\bar{q}}(\boldsymbol{k}, \boldsymbol{k}', z) = \frac{\alpha_s}{2\pi \pi_\epsilon} n_f \mathcal{P}_{qg}(z,\epsilon) \frac{1}{\boldsymbol{q}^2} \left[\frac{C_f}{C_a} + z(1-z) \frac{\boldsymbol{q} \cdot \boldsymbol{\Delta}}{\boldsymbol{\Delta}^2} \right], \tag{38}$$

11

where the overall factor $1/2$ for the gg final state stems from the indistinguishability of identical bosons in the final state.

If we parametrize the momentum fraction z in terms of the rapidity difference $\Delta y \equiv y_p - q_q$ of the final state gluons, *i.e.*

$$z = \frac{e^{\Delta y}}{(\boldsymbol{k'}^2/\boldsymbol{q}^2) + e^{\Delta y}}, \tag{39}$$

we can see that F_{ggg} reduces in the limits $\Delta y \to \pm\infty$ (including the corresponding Jacobian factor) to half of the central production vertex of Eq. (31). To regularize the resulting divergence of the rapidity integral we introduce a lower bound $|\Delta y| > -\eta_b$, where η_b is again taken in the limit $\eta_b \to -\infty$, and define $\mathcal{F}_{ggg}(\boldsymbol{k}, \boldsymbol{k'}, z, \eta_b) = F_{ggg}(\boldsymbol{k}, \boldsymbol{k'}, z)\Theta(|\Delta y| + \eta_b)$. As in the case of virtual corrections it is now needed to subtract the contribution from gluon production at central rapidities to construct the complete differential cross section, schematically:

$$\tag{40}$$

This leads to the definition of the coefficient

$$\mathcal{G}_{ggg}^{(a)}(\boldsymbol{k}, \boldsymbol{k'}, z, \eta_b) = \mathcal{F}_{ggg}(\boldsymbol{k}, \boldsymbol{k'}, z, \eta_b) - \frac{1}{2}\left[\frac{1}{z}\mathcal{V}(\boldsymbol{k}, \boldsymbol{k'}; \boldsymbol{q}; \eta_a, \eta_b) + \frac{1}{1-z}\mathcal{V}(\boldsymbol{k}, \boldsymbol{q}; \boldsymbol{k'}; \eta_a, \eta_b)\right]. \tag{41}$$

Defining finally the cross-section for quasi-elastic production as

$$d\hat{\sigma}_{ab}^{(qea)} = h_{a,\text{gluon}}^{(0)}(\boldsymbol{k'})\mathcal{G}_{ggg}^{(a)}(\boldsymbol{k}, \boldsymbol{k'}, z, \eta_b)h_{b,\text{gluon}}^{(0)} \, dz \, d^{2+2\epsilon}\boldsymbol{k} \, d^{2+2\epsilon}\boldsymbol{k'}, \tag{42}$$

the sum of central and quasi-elastic contributions,

$$d\hat{\sigma}_{ab} = d\hat{\sigma}_{ab}^{(c)} + d\hat{\sigma}_{ab}^{(qea)} + d\hat{\sigma}_{ab}^{(qeb)}, \tag{43}$$

turns out to be finite, if integrated over the gluon rapidity, with a well-defined limit $\eta_{a,b} \to \pm\infty$. This completes our calculation of the gluon-initiated forward jet vertex at NLO using the high energy effective action constructed by Lipatov.

IV   Conclusions and Outlook

We have performed the calculation of the forward jet vertex at next-to-leading order in the BFKL formalism, offering an explicit derivation of the gluon-initiated contribution. This adds to the previously calculated for the quark-initiated vertex and completes the derivation of the full vertex. We have found agreement with previous results in the literature. Our method of calculation is based on the high energy effective action for QCD proposed by Lipatov, which is proven to be very useful to streamline our calculations. Our subtraction and regularization procedure in order to avoid over-counting of kinematic regions has been proven to work well in both gluon and quark

cases. Compared to more standard calculations, in this approach the number of Feynman diagrams finally contributing to the physical observables is reduced and gauge invariance is readily ensured. We are now confident this method will help in the calculation of further amplitudes at loop level. We understand that it is important to test these high energy resummations in exclusive observables at the Large Hadron Collider. Typical pro- cesses where our approach can be applied include the inclusive production of a pair of forward (Mueller-Navelet) jets. Similar techniques are now being used to calculate the production of a forward jet coupled to a color singlet, associated to diffractive events (Mueller-Tang jets) [25] at next-to-leading order.

Acknowledgments

A   Appendix

In the following we present further details on the NLO calculation of both virtual and real correc- tions

A.1   Virtual corrections

We refer for the notation to Fig. 4. Tadpole contributions vanish in dimensional regularization. The contribution for each of these diagrams can be written in terms of master integrals labelled with the following notation: M, S, P, and Q denote, respectively, the existence of a propagator of the form $k^+(\to b \cdot k), k^2, (k-p_a)^2$ or $(k-q)^2$. The number at the end $(0, 1, 2,$ or $3)$ indicates how many tensor indices are present in the numerator (*e.g.* 2 stands for a factor $k^\mu k^\nu$). $\xi = a^2 = b^2 = 4e^{-\rho}$ are chosen to indicate the squares of the new light-cone vectors. For diagrams (E), (F), (I) and (J) in Fig. 4 the contribution with reversed arrows is included. Diagrams (G) and (H) turn out to vanish completely. The symmetry factors for the diagrams, which are included, are equal to one apart from diagrams (C) and (D), for which it is two. In more detail, these are all the contributing

expressions:

$$i\mathcal{M}_{(A)} = -\frac{ig^3}{2}\boldsymbol{q}^2 f_{abc}\, N_c \int \frac{d^d k}{(2\pi)^d} \frac{(k^+ - 2p_a^+)^2\, \varepsilon \cdot \varepsilon^* + 4\,\xi\, \varepsilon \cdot k\, \varepsilon^* \cdot (k-q)}{k^+ k^2 (k-p_a)^2 (k-q)^2}$$

$$= -\frac{ig^3}{2}\boldsymbol{q}^2 f_{abc}\, N_c \left\{ 16 e^{-\rho}\varepsilon_\mu \varepsilon_\nu^*[\text{MSPQ2}] - 16 e^{-\rho}\varepsilon^* \cdot q\, \varepsilon_\mu[\text{MSPQ1}] - 4p_a^+ \varepsilon \cdot \varepsilon^*[\text{SPQ0}]\right.$$

$$\left. + 4(p_a^+)^2 \varepsilon \cdot \varepsilon^*[\text{MSPQ0}] + (n^+)_\mu \varepsilon \cdot \varepsilon^*[\text{SPQ1}]\right\};$$

$$i\mathcal{M}_{(B)} = -\frac{ig^3}{2} f_{abc}\, N_c \int \frac{d^d k}{(2\pi)^d} \frac{1}{k^2(k-p_a)^2(k-q)^2}[4p_a^+\{\varepsilon \cdot \varepsilon^*((k-p_a)^2 - \boldsymbol{q}^2)$$

$$+ 4(\varepsilon \cdot k\, \varepsilon^* \cdot q - \varepsilon \cdot q\, \varepsilon^* \cdot k)\} + k^+\{7\boldsymbol{q}^2 \varepsilon \cdot \varepsilon^* + (18 + 16\epsilon)\varepsilon \cdot k\, \varepsilon^* \cdot (k-q)$$

$$+ 16\,\varepsilon \cdot q\, \varepsilon^* \cdot q\}]$$

$$= -\frac{ig^3}{2} f_{abc}\, N_c\{(18 + 16\epsilon)(n^+)_\mu \varepsilon_\nu \varepsilon_\rho^*[\text{SPQ3}] - (18 + 16\epsilon)(n^+)_\mu \varepsilon_\nu\, \varepsilon^* \cdot q[\text{SPQ2}]$$

$$+ [(n^+)_\mu(16\varepsilon \cdot q\, \varepsilon^* \cdot q + 7\boldsymbol{q}^2 \varepsilon \cdot \varepsilon^*) - 16p_a^+(\varepsilon \cdot q\, \varepsilon_\mu^* - \varepsilon^* \cdot q\, \varepsilon_\mu)][\text{SPQ1}]$$

$$- 4p_a^+\boldsymbol{q}^2 \varepsilon \cdot \varepsilon^*[\text{SPQ0}] + 4p_a^+ \varepsilon \cdot \varepsilon^*[\text{SQ0}]\};$$

14

$$i\mathcal{M}_{(\mathrm{C})} = -\frac{ig^3}{2} f_{abc} N_c \int \frac{d^d k}{(2\pi)^d} \frac{1}{k^+ k^2 (k-q)^2} [4\xi(\varepsilon \cdot k\, \varepsilon^* \cdot q - \varepsilon \cdot q\, \varepsilon^* \cdot k)$$
$$+ \varepsilon \cdot \varepsilon^* (4k^+ p_a^+ + \xi(2(k-p_a)^2 - \boldsymbol{q}^2)]$$
$$= -\frac{ig^3}{2} f_{abc} N_c \{-16 e^{-\rho}(\varepsilon \cdot \varepsilon^* p_{a\mu} + \varepsilon \cdot q\, \varepsilon_\mu^* - \varepsilon^* \cdot q\, \varepsilon_\mu)[\mathrm{MSQ1}]$$
$$- 4 e^{-\rho} \boldsymbol{q}^2 \varepsilon \cdot \varepsilon^* [\mathrm{MSQ0}] + 4 p_a^+ \varepsilon \cdot \varepsilon^* [\mathrm{SQ0}]\};$$

$$i\mathcal{M}_{(\mathrm{D})} = \frac{ig^3}{2\boldsymbol{q}^2} f_{abc} N_c \int \frac{d^d k}{(2\pi)^d} \frac{1}{k^2 (k-q)^2} [-8 p_a^+ \boldsymbol{q}^2 \varepsilon \cdot \varepsilon^* + (5+4\epsilon)k^+ \{\varepsilon \cdot \varepsilon^* (\boldsymbol{q}^2$$
$$- 2(k-p_a)^2) + 4\varepsilon \cdot q\, \varepsilon^* \cdot k - 4\varepsilon \cdot k\, \varepsilon^* \cdot q\}]$$
$$= \frac{ig^3}{2\boldsymbol{q}^2} f_{abc} N_c \{(20+16\epsilon)(n^+)_\mu (\varepsilon \cdot q\, \varepsilon_\nu^* - \varepsilon^* \cdot q\, \varepsilon_\nu + \varepsilon \cdot \varepsilon^* p_{a\nu})[\mathrm{SQ2}]$$
$$+ (5+4\epsilon)\boldsymbol{q}^2 \varepsilon \cdot \varepsilon^* (n^+)_\mu [\mathrm{SQ1}] - 8 p_a^+ \boldsymbol{q}^2 \varepsilon \cdot \varepsilon^* [\mathrm{SQ0}]\};$$

$$i\mathcal{M}_{(\mathrm{E})} = \frac{2ig^3}{\boldsymbol{q}^2} f_{abc} n_f \int \frac{d^d k}{(2\pi)^d} \frac{1}{k^2 (k-q)^2} [p_a^+ \boldsymbol{q}^2 \varepsilon \cdot \varepsilon^* + k^+ [\varepsilon \cdot \varepsilon^* (2(k-p_a)^2 - \boldsymbol{q}^2)$$
$$+ 4(\varepsilon \cdot k\, \varepsilon^* \cdot q - \varepsilon \cdot q\, \varepsilon^* \cdot k)]]$$
$$= -\frac{2ig^3}{\boldsymbol{q}^2} f_{abc} n_f \{4(n^+)_\mu (\varepsilon \cdot q\, \varepsilon_\nu^* - \varepsilon^* \cdot q\, \varepsilon_\nu + \varepsilon \cdot \varepsilon^* p_{a\nu})[\mathrm{SQ2}]$$
$$+ \varepsilon \cdot \varepsilon^* \boldsymbol{q}^2 (n^+)_\mu [\mathrm{SQ1}] - p_a^+ \boldsymbol{q}^2 \varepsilon \cdot \varepsilon^* [\mathrm{SQ0}]\};$$

$$i\mathcal{M}_{(\mathrm{F})} = \frac{ig^3}{2\boldsymbol{q}^2} f_{abc} N_c \int \frac{d^d k}{(2\pi)^d} \frac{k^+}{k^2 (k-q)^2} [\varepsilon \cdot \varepsilon^* (2(k-p_a)^2 - \boldsymbol{q}^2)$$
$$+ 4(\varepsilon \cdot k\, \varepsilon^* \cdot q - \varepsilon \cdot q\, \varepsilon^* \cdot k)]$$
$$= -\frac{ig^3}{2\boldsymbol{q}^2} f_{abc} N_c \{4(n^+)_\mu (\varepsilon \cdot \varepsilon^* p_{a\nu} + \varepsilon \cdot q\, \varepsilon_\nu^* - \varepsilon^* \cdot q\, \varepsilon_\nu)[\mathrm{SQ2}]$$
$$+ \boldsymbol{q}^2 \varepsilon \cdot \varepsilon^* (n^+)_\mu [\mathrm{SQ1}]\};$$

$$i\mathcal{M}_{(\mathrm{I})} = ig^3 f_{abc} n_f \int \frac{d^d k}{(2\pi)^d} \frac{1}{k^2 (k-p_a)^2 (k-q)^2} [p_a^+ (-\boldsymbol{q}^2 \varepsilon \cdot \varepsilon^*$$
$$+ 2(\varepsilon \cdot k\, \varepsilon^* \cdot q - \varepsilon \cdot q\, \varepsilon^* \cdot k)) + k^+ (\varepsilon \cdot \varepsilon^* (\boldsymbol{q}^2 - 2(k-p_a)^2)$$
$$+ 8\varepsilon \cdot k\, \varepsilon^* \cdot (k-q) + 2\varepsilon \cdot q\, \varepsilon^* \cdot q)]$$
$$= ig^3 f_{abc} n_f \{8(n^+)_\mu \varepsilon_\nu \varepsilon_\rho^* [\mathrm{SPQ3}] - 8\varepsilon^* \cdot q (n^+)_\mu \varepsilon_\nu [\mathrm{SPQ2}]$$
$$+ [(\boldsymbol{q}^2 \varepsilon \cdot \varepsilon^* + 2\varepsilon \cdot q\, \varepsilon^* \cdot q)(n^+)_\mu + 2 p_a^+ \varepsilon^* \cdot q\, \varepsilon_\mu - 2 p_a^+ \varepsilon \cdot q\, \varepsilon_\mu^*][\mathrm{SPQ1}]$$
$$- \boldsymbol{q}^2 p_a^+ \varepsilon \cdot \varepsilon^* [\mathrm{SPQ0}]\};$$

$$i\mathcal{M}_{(\mathrm{J})} = ig^3 f_{abc} N_c \int \frac{d^d k}{(2\pi)^d} \frac{k^+}{k^2 (k-p_a)^2 (k-q)^2} \varepsilon \cdot k\, \varepsilon^* \cdot (k-q)$$
$$= ig^3 f_{abc} N_c (n^+)_\mu \{\varepsilon_\nu \varepsilon_\rho^* [\mathrm{SPQ3}] - \varepsilon^* \cdot q\, \varepsilon_\nu [\mathrm{SPQ2}]\}.$$

Those integrals which are not suppressed in the $\rho \to \infty$ limit are:

$$[\text{SQ0}] = \frac{i}{(4\pi)^{2+\epsilon}}(\boldsymbol{q}^2)^\epsilon \frac{\Gamma(-\epsilon)\Gamma^2(1+\epsilon)}{\Gamma(2+2\epsilon)};$$

$$[\text{SQ2}] = (g^{\mu\nu}\boldsymbol{q}^2 + q^\mu q^\nu(4+2\epsilon))\frac{1}{4(3+2\epsilon)}\,[\text{SQ0}]\,;$$

$$[\text{SPQ0}] = \frac{1+2\epsilon}{\epsilon\boldsymbol{q}^2}\,[\text{SQ0}]\,;$$

$$[\text{SPQ1}] = \left(q^\mu + \frac{1}{\epsilon}p_a^\mu\right)[\text{SQ0}]\,;$$

$$[\text{SPQ2}] = \left\{\frac{1}{2+2\epsilon}\left[\frac{1}{2}g^{\mu\nu} + \left(\frac{q^\mu p_a^\nu + p_a^\mu q^\nu}{\boldsymbol{q}^2}\right) + \frac{2}{\epsilon}\frac{p_a^\mu p_a^\nu}{\boldsymbol{q}^2}\right] + \frac{1}{\boldsymbol{q}^2}q^\mu q^\nu\right\}[\text{SQ0}]\,;$$

$$[\text{SPQ3}] = \frac{1}{\epsilon(1+\epsilon)(3+2\epsilon)}\left\{\frac{1}{\boldsymbol{q}^2}\left[p_a^\mu p_a^\nu p_a^\rho + \epsilon q^\mu p^\nu p^\rho + \frac{1}{2}\epsilon(1+\epsilon)q^\mu q^\nu p^\rho\right.\right.$$

$$\left.- \frac{1}{6}(1-\epsilon)(2+\epsilon)^2 q^\mu q^\nu q^\rho\right] + \frac{\epsilon}{4}\left[p^\mu g^{\nu\rho} + (1+\epsilon)q^\mu g^{\nu\rho}\right]$$

$$+ \text{ cyclic permutations of } \mu, \nu \text{ and } \rho\Bigg\}[\text{SQ0}]\,;$$

$$[\text{MSQ1}] = \frac{b^\mu}{\xi}\,[\text{SQ0}] + \frac{1}{2}q^\mu\left\{\frac{-i}{(4\pi)^{2+\epsilon}}\frac{\Gamma^2\left(\frac{1}{2}+\epsilon\right)\Gamma\left(\frac{1}{2}-\epsilon\right)\Gamma\left(\frac{1}{2}\right)}{\Gamma(1+2\epsilon)(\boldsymbol{q}^2)^{\frac{1}{2}-\epsilon}\xi^{\frac{1}{2}}}\right\};$$

$$[\text{MSPQ0}] = -\frac{i}{(4\pi)^{2+\epsilon}}\frac{(\boldsymbol{q}^2)^{\epsilon-1}}{p_a^+}\frac{\Gamma(1-\epsilon)\Gamma^2(\epsilon)}{\Gamma(2\epsilon)}\left(\ln\left[\frac{p_a^+}{|\boldsymbol{q}|}\right] + \frac{\rho}{2} + \frac{\psi(1)-2\psi(\epsilon)+\psi(1-\epsilon)}{2}\right).$$

A.2 Details on the real corrections

We refer to Figs. 7 and 8 for our notation. We have

$$p^- = \frac{(\boldsymbol{k}-\boldsymbol{q})^2}{(1-z)p_a^+}, \quad k^- = \frac{(\boldsymbol{q}-z\boldsymbol{k})^2 + z(1-z)\boldsymbol{k}^2}{z(1-z)p_a^+}. \tag{44}$$

Within the given choice of polarization vectors, diagrams (a), (b), (c), (d) and (i) are immediately zero, while diagram (h) turns out to vanish as well. The amplitudes for the non-vanishing diagrams can be written in the following form

$$i\mathcal{M}_{(\text{e})} = \varepsilon_{a\mu}\varepsilon_{b\nu}^*\varepsilon_{c\rho}^* 2ig^2\frac{f_{ade}f_{bce}}{s}p_a^+\left\{g^{\nu\rho}[k^\mu(1-2z)-p^\mu+q^\mu] + g^{\mu\nu}(2p^\rho+q^\rho)\right.$$

$$\left. - g^{\mu\rho}(2q^\nu+p^\nu)\right\};$$

$$i\mathcal{M}_{(\text{f})} = \varepsilon_{a\mu}\varepsilon_{b\nu}^*\varepsilon_{c\rho}^*(-ig^2)\frac{f_{abe}f_{cde}}{t}p_a^+\left\{-4z(g^{\nu\rho}p^\mu+g^{\mu\rho}p_a^\nu) + g^{\mu\nu}[k^\rho(2-z)+p^\rho(2+z)\right.$$

$$\left. + p_a^\rho(-2+3z)]\right\};$$

16

$$i\mathcal{M}_{(g)} = \varepsilon_{a\mu}\varepsilon_{b\nu}^*\varepsilon_{c\rho}^*(-ig^2)\frac{f_{ace}f_{bde}}{u}p_a^+\bigg\{ -4(1-z)[g^{\mu\nu}p_a^\rho + g^{\nu\rho}q^\mu] + g^{\mu\rho}[k^\nu(1+z)$$

$$+ p_a^\nu(1-3z) + q^\nu(3-z)]\bigg\};$$

$$i\mathcal{M}_{(j)} = -\frac{2g^2 f_{acd}\, t^c}{s}\varepsilon_{a\mu}[k^\mu(n^+)^\sigma - p_a^+ g^{\mu\sigma}]\bar{u}(p)\gamma_\sigma v(q);$$

$$i\mathcal{M}_{(k)} = -\frac{ig^2\, t^d t^a}{u}\varepsilon_{a\mu}\bar{u}(p)\slashed{n}^+(\slashed{p}_a - \slashed{q})\gamma^\mu v(q);$$

$$i\mathcal{M}_{(l)} = \frac{ig^2\, t^a t^d}{t}\varepsilon_{a\mu}\bar{u}(p)\gamma^\mu(\slashed{p}_a - \slashed{p})\slashed{n}^+ v(q).$$

(45)

References

[1] L. N. Lipatov, Nucl. Phys. B **452** (1995) 369 [hep-ph/9502308].

[2] M. Hentschinski and A. Sabio Vera, Phys. Rev. D **85** (2012) 056006 [arXiv:1110.6741 [hep-ph]].

[3] V. S. Fadin and L. N. Lipatov, Nucl. Phys. B **406** (1993) 259.

[4] V. S. Fadin and R. Fiore, Phys. Lett. B **294**, 286 (1992).

[5] L. N. Lipatov, Phys. Rept. **286** (1997) 131 [hep-ph/9610276].

[6] V. Del Duca and C. R. Schmidt, Phys. Rev. D **57** (1998) 4069 [hep-ph/9711309].

[7] M. Ciafaloni and D. Colferai, Nucl. Phys. B **538** (1999) 187 [hep-ph/9806350].

[8] V. S. Fadin, R. Fiore, M. I. Kotsky and A. Papa, Phys. Rev. D **61** (2000) 094005 [hep-ph/9908264].

[9] J. Bartels, D. Colferai and G. P. Vacca, Eur. Phys. J. C **24** (2002) 83 [hep-ph/0112283].

[10] J. Bartels, D. Colferai and G. P. Vacca, Eur. Phys. J. C **29** (2003) 235 [hep-ph/0206290].

[11] A. Sabio Vera, Nucl. Phys. B **746** (2006) 1 [hep-ph/0602250].

[12] A. Sabio Vera and F. Schwennsen, Nucl. Phys. B **776** (2007) 170 [hep-ph/0702158 [HEP-PH]].

[13] C. Marquet and C. Royon, Phys. Rev. D **79** (2009) 034028 [arXiv:0704.3409 [hep-ph]].

[14] A. Sabio Vera and F. Schwennsen, Phys. Rev. D **77** (2008) 014001 [arXiv:0708.0549 [hep-ph]].

[15] M. Deak, F. Hautmann, H. Jung and K. Kutak, JHEP **0909** (2009) 121 [arXiv:0908.0538 [hep-ph]].

[16] D. Colferai, F. Schwennsen, L. Szymanowski and S. Wallon, JHEP **1012** (2010) 026 [arXiv:1002.1365 [hep-ph]].

[17] F. Caporale, D. Y. .Ivanov, B. Murdaca, A. Papa and A. Perri, JHEP **1202** (2012) 101 [arXiv:1112.3752 [hep-ph]].

[18] D. Y. .Ivanov and A. Papa, JHEP **1205** (2012) 086 [arXiv:1202.1082 [hep-ph]].

[19] D. Y. .Ivanov and A. Papa, JHEP **1207** (2012) 045 [arXiv:1205.6068 [hep-ph]].

[20] F. Caporale, D. Y. .Ivanov, B. Murdaca and A. Papa, arXiv:1211.7225 [hep-ph].

[21] G. Chachamis, M. Hentschinski, J. D. Madrigal Martinez and A. Sabio Vera, Nucl. Phys. B **861** (2012) 133 [arXiv:1202.0649 [hep-ph]].

[22] G. Chachamis, M. Hentschinski, J. D. M. Martinez and A. Sabio Vera, arXiv:1211.2050 [hep-ph].

[23] G. Chachamis, M. Hentschinski, J. D. Madrigal and A. Sabio Vera, arXiv:1206.5101 [hep-ph].

[24] V. S. Fadin, R. Fiore, M. I. Kotsky and A. Papa, Phys. Rev. D **61** (2000) 094006 [hep-ph/9908265].

[25] M. Hentschinski, B. Murdaca and A. Sabio Vera, in preparation; arXiv:1206.1622 [hep-ph]. M. Hentschinski, B. Murdaca, Proceedings of Diffraction 2012: International Workshop on Diffraction in High-Energy Physics (Diffraction), 10-15 Sep 2012. Puerto del Carmen, Lanzarote, Canary Islands, Spain.